2010

CONFINING AN ORGANIC MOLECULE IN A NANOCAVITY: EFFECT ON ROTATIONAL/VIBRATIONAL MOTION AND ITS CONSEQUENCE FOR SPIN DEPHASING.

Lopamudra Das
Virginia Commonwealth University

Virginia Commonwealth University

This is to certify that the thesis prepared by Lopamudra Das entitled
CONFINING AN ORGANIC MOLECULE IN A NANOCAVITY: EFFECT ON ROTATIONAL/VIBRATIONAL MOTION AND ITS CONSEQUENCE FOR SPIN DEPHASING
has been approved by her committee as satisfactory completion of the thesis or dissertation requirement for the degree of Master's of Science.

Dr.Supriyo Bandyopadhyay, Professor, Virginia Commonwealth University.

Dr. Gary M Atkinson , Associate Professor, Virginia Commonwealth University.

Dr.Gary Tepper, Professor, Virginia Commonwealth University.

Dr. Ashok Iyer, Department Chair, Department of Electrical and Computer Engineering

Dr. Rosalyn Hobson, Associate Dean, School of Engineering

Dr. F. Douglas Boudinot, Dean of the School of Graduate Studies

August 13, 2010

CONFINING AN ORGANIC MOLECULE IN A NANOCAVITY: EFFECT ON ROTATIONAL/VIBRATIONAL MOTION AND ITS CONSEQUENCE FOR SPIN DEPHASING

A Thesis submitted in partial fulfillment of the requirements for the degree of Master of Science at Virginia Commonwealth University.

by

LOPAMUDRA DAS
M.Tech. Jadavpur University, India, 2004
B.Tech. University of Kalyani, India, 2002

Director: SUPRIYO BANDYOPADHYAY
PROFESSOR, DEPARTMENT OF ELECTRICAL AND COMPUTER ENGINEERING

Virginia Commonwealth University
Richmond, Virginia
August 2010.

Acknowledgement

The work described in the report would not have been possible without the constant support and encouragement of the following people to whom I am very grateful and would like to sincerely thank them for all their assistance.

My advisor Prof.Supriyo Bandyopadhyay, for giving me the opportunity to work in his group, his invaluable help and advice throughout my graduate studies and his expert guidance in my research work, as well as his kind encouragement and patient understanding.

US National Science Foundation, for providing the financial support to carry out this project.

My committee members Dr.Gary Atkinson and Dr. Gary Tepper for agreeing to be on my committee.

Prof. Gary Atkinson for his valuable advice and support all throughout my studies at VCU and for providing his laboratory resources.

Dr.Dmitry Pestov for his kind assistance and advice.

The department secretaries Ms.Dorothy Kelly and Ms. Caitlin Bergandahl for their help with purchases and administrative work.

My colleague and best friend Jennette Mateo who has been my pillar of support in my research work as well as personal life from the time we met and without whom life at VCU would have been very different.

My colleague and friend Pratik Agnihotri for all his assistance and generous cooperation during my trying experiments.

My friends Lynn Myint ,Ravi Rastogi, Aric Hackebill, Kakali Sen, Soumya Remesh , my senior colleague Dr.Bhargava Kanchibotla and all my numerous other friends and well wishers for being there for me through the ups and downs of life during my stay in the U.S, and young Saumil for being so helpful and nice.

Prof.Sukumar Basu for his constant motivation and valuable advice from the very beginning.

My ma and baba for their unending love and support, and also my ma for being my inspiration.

Last, but not the least I would like to thank everyone who has helped me reach here. Above all I would thank God for all the blessings without which nothing would have been possible.

Contents

List of Figures

Page

Abstract

CONFINING AN ORGANIC MOLECULE IN A NANOCAVITY: EFFECT ON ROTATIONAL/VIBRATIONAL MOTION AND ITS CONSEQUENCE FOR SPIN DEPHASING

By Lopamudra Das

A thesis submitted in partial fulfillment of the requirements for the degree of Master of Science at Virginia Commonwealth University.

Virginia Commonwealth University, 2010.

Major Director: Dr.Supriyo Bandyopadhyay.
Professor, Department of Electrical and Computer Engineering

Recently, it was found that the temperature-dependent spin dephasing time of localized electrons in the organic molecule tris(8-hydroxyquinoline aluminum), or Alq_3, increases significantly when the molecule is confined within 1-2 nm sized nanocavities. This was thought to be due to weakening of spin-phonon coupling within the nanocavity, which would suppress dephasing. However, it is also possible that confinement quenches some of the rotational/vibrational modes of the molecule, leading to suppression of spin coupling with these modes and a concomitant increase in the spin dephasing time. To test this possibility, we have carried out infrared spectroscopy of Alq_3 molecules confined within 1-2 nm sized nanovoids in porous alumina films. The spectra show absence of the sharp peaks associated with hydrogen stretching modes in bulk powders, indicating that confinement indeed quenches these modes. This has profound consequences for spin-based quantum computing paradigms predicated on the use of organic molecules as hosts for qubits.

CHAPTER 1 Introduction

There is significant current interest in understanding the relaxation mechanisms of both ensembles of spins[1-3] and single spins[4, 5] in organic molecules owing to the promise of organic spintronics[6, 7]. Of particular interest are the *dephasing* mechanisms of a single spin in an organic molecule[5, 8] since these molecules can be excellent hosts for spin-based qubits[5]. When used in quantum gates, organic molecules should exhibit superb gate fidelity[9] and there exists a unique and elegant scheme for spin qubit read-out that has no parallel in inorganic systems[5]. As a result, understanding the mechanisms for spin dephasing in organic molecules has assumed added importance.

In the past, we found two important results: (1) the ensemble averaged spin dephasing time (T_2^* time) of bound electrons in the organic molecule tris-(8-hydroxyquinoline aluminum), or *Alq3* ($C_{27}H_{18}N_3O_3Al$), goes up by ~ 2.5 times in the temperature range 4.2 K – 100 K compared to the T_2^* time in bulk powder[5]; and (2) the T_2^* time decreases rapidly with increasing temperature, leading us to believe that dephasing is mediated by spin interaction with time-dependent perturbations such as phonons and molecular vibrations[5]. Since these interactions are inelastic, they are much more effective than elastic interactions in dephasing spin.

It is obvious that interactions with time-dependent perturbations are suppressed within a nanocavity, but what these perturbations are, and what causes the suppression,

were not understood. One possibility is that the time-dependent perturbations are acoustic phonons and the nanocavity confines them and discretizes their energies[10]. In that case, spin-phonon interaction will be suppressed if phonons of the right energies that can induce transitions between anti-parallel spin states are not allowed within the cavity owing to boundary conditions. One could think of this as a non-traditional phonon bottleneck effect, somewhat different from the traditional one[11]. Another possibility is that molecules can form dimers and multimers in bulk powder and experience enhanced electron-phonon interaction[12]. Within nanocavities however, they can only form monomers and the electron-phonon interaction is reduced. Yet another possibility is that confinement within the nanocavity affects the vibrational and rotational modes of the molecules themselves, which changes their characteristic frequencies, making them increasingly off-resonant with spin splitting energies within the molecule. This would make them ineffective in inducing transitions between anti-parallel spin states, resulting in an increase in the spin dephasing time. In this thesis, we have explored this last possibility.

CHAPTER 2 Objective and Experimental Method

2.1 Introduction

In order to fabricate the nanocavities, we followed the method of ref. 11. We first anodized a 99.999% pure aluminum foil of 0.1 mm thickness in 15% sulfuric acid at 10 V dc (at room temperature) to produce a porous alumina film containing pores of diameter 10 nm on the surface[13]. There are cracks of diameter 1-2 nm in the pore walls[11, 14, 15] that end in a small nanovoid of 1-2 nm diameter. Ref. 5 contains a transmission electron micrograph of such a crack. The nanovoids act as "nanocavities". Because their linear dimensions are 1-2 nm, only one or two molecules can be accommodated within any nanovoid.

2.2 Sample preparation

Anodized Aluminium Oxide (AAO) has been widely used as a convenient template for fabrication of highly ordered arrays of nanostructures. The template is obtained by anodization of pure aluminium sheets in a suitable acid and voltage, resulting in the formation of a nanoporous film on the surface.. The pore diameter can be controllably varied from 8 nm to few hundred nm by using different acids for anodization, and the pore density ranges from 10^{10}-10^{12} pores /cm.^{2}.Using a multi step anodization process, a very uniform honeycomb pattern of nanopores can be created in the alumina matrix.While

commercially available aluminum sheets can be anodized to produce nanoporous films, typically such sheets have surface roughness in the order of few hundreds of nanometers. Direct anodization of such a surface would result in non uniform dissolution of aluminum during anodization and adversely affect pore regimentation. Hence as purchased aluminium sheets are first electro polished to obtain a very smooth mirror like surface and then anodized. Thus there are two main steps in the fabrication of the porous alumina template, electro polishing and anodization.

2.2 Electropolishing

Highly pure (99.998% pure), 100 μm thick aluminum foils are diced into one inch square coupons to facilitate handling. Electropolishing is then carried out using Leeco L1 electrolyte consisting of a solution of 90cc perchloric acid,150cc butyl cellusolve, 1050cc ethanol and 250ml distilled water for ~ 10 seconds and applying 40 V dc in a commercially available electropolisher Electromet-4 (Buehler Ltd).The aluminium foil is placed at the anode and the area exposed to the Leeco solution is electropolished. Perchloric acid is the etchant for aluminum. Ethanol and butyl cellusolve are polarizable molecules which sheath the crest regions on the surface that have the highest electric fields as a result of which troughs on the surface dissolve faster. This effect is counter balanced by the fact that mass transport of Al^{3+} ions from the crests is more efficient. The interplay of these two effects results in the formation of ridges on the surface. The surface roughness is reduced from hundreds of nanometers to around 3 nanometers. Atomic Force Microscopy of the surface

reveals an egg-carton pattern which has features 30-50 nm in diameter and around 3-5 nm in height. These periodic patterns act as nucleation sites for the self assembly of nanopores.

2.3 Anodization of aluminium to form nanoporous templates

Anodization of the electropolished alumina surface yields a porous alumina structure on the surface of the foil. The anodization is carried out in a commercially available electrochemical cell schematically shown in Figure2.1. The aluminium foil is the anode and a platinum grid is used as the cathode. Platinum is used because it does not react with the acids used as the electrolyte. Typically the acids used for anodization are 3% Oxalic acid or 15% Sulfuric acid. A regulated power supply provides a highly stable DC voltage for anodization. Anodization is done by passing direct current because anodic alumina allows current to flow in one direction only.Anodization of aluminium sheets in 15% sulfuric acid at 10V DC yields nanopores of 10 nm diameters respectively. Scanning electron micrograph of the sample cross section is given in Figure 2.2.

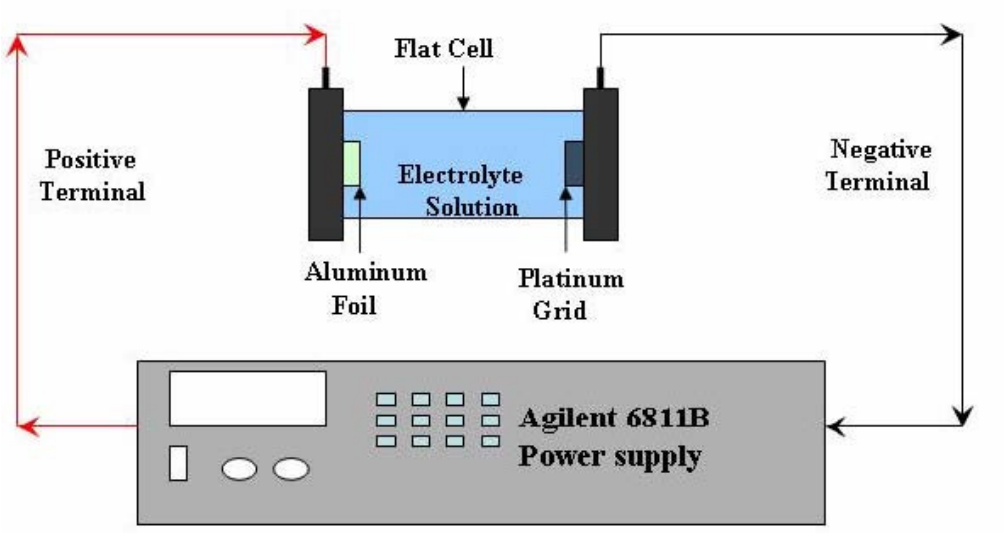

Figure 2.1: Schematic diagram of the experimental setup for anodization. (Courtesy of Bhargava Kanchibotla PhD Thesis)

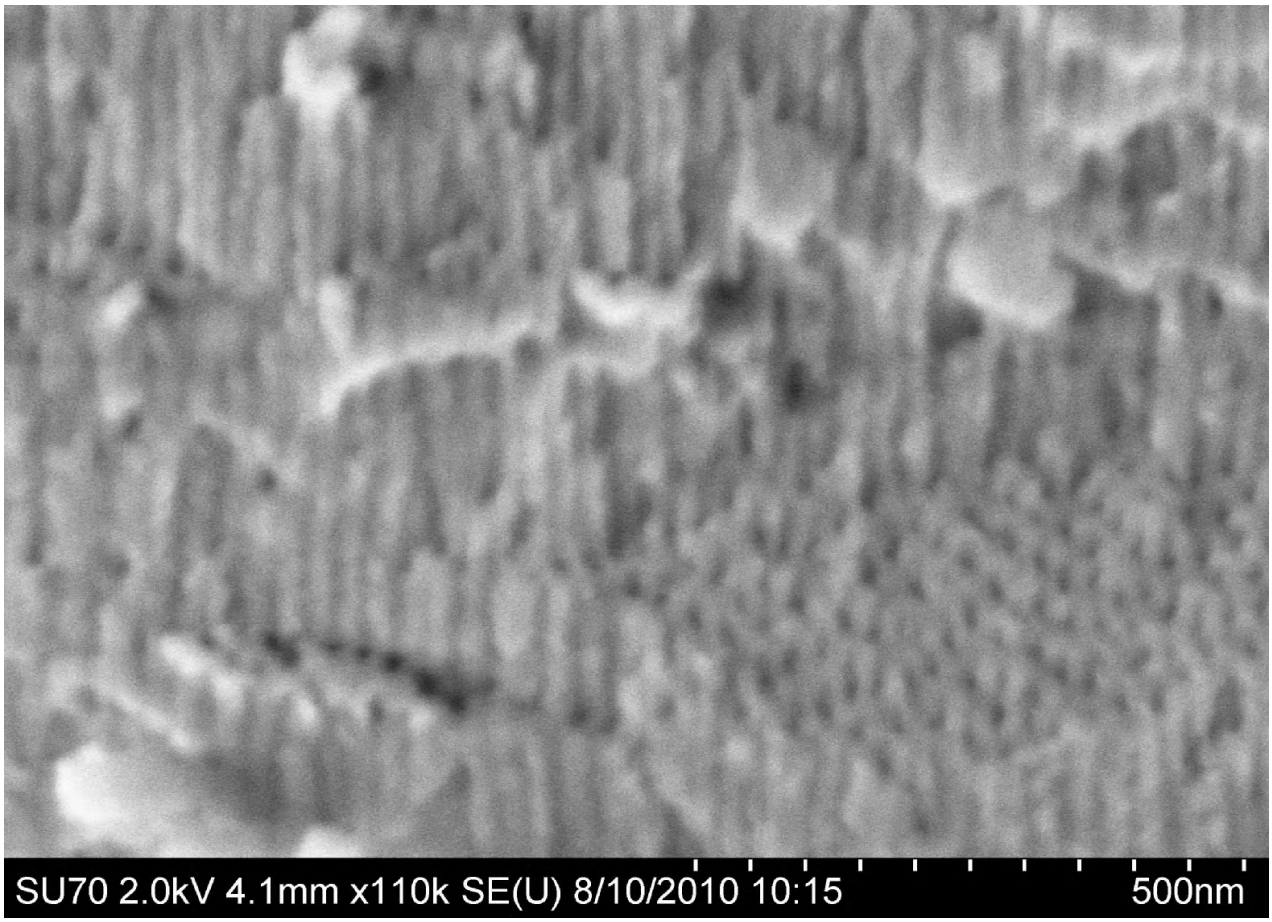

Fig 2.2: SEM cross sectional image of a sample anodized in 15% sulfuric acid at 10V DC.

2.4 Chemical processes involved in the formation of nanopores

The chemical reactions occurring during anodization are as follows:

At the Anode:

Oxidation of Aluminum: $2Al + 3H_2O = Al_2O_3 + 6H^+ + 6e^-$

Dissolution of Alumina: $Al_2O_3 + 6H^+ = 2Al^{3+} + 3H_2O$

At the Cathode:

Hydrogen Evolution: $6H^+ + 6e^- = 3H_2$

Several theoretical models have been proposed to explain the process of pore growth. The model proposed by O'Sullivan et al which is based on inhomogeneous electric field distribution at pore tips and field assisted dissolution explains why pores grow and what determines the size distribution of the pores. It was shown that parameters like the pore diameter, the interpore separation and the steady state barrier layer thickness are directly proportional to the applied voltage.

Again the model developed by Jessensky et al tried to explain densely packed hexagonal pore structure developed under special anodization conditions. The forces between the neighboring pores in the hexagonal structure are due to the mechanical stress produced by the volume expansion that occurs during the conversion of aluminum to alumina. According to this model, the voltage and the electrolyte composition influence the relative thickness of the porous alumina layer compared to the consumed aluminum.

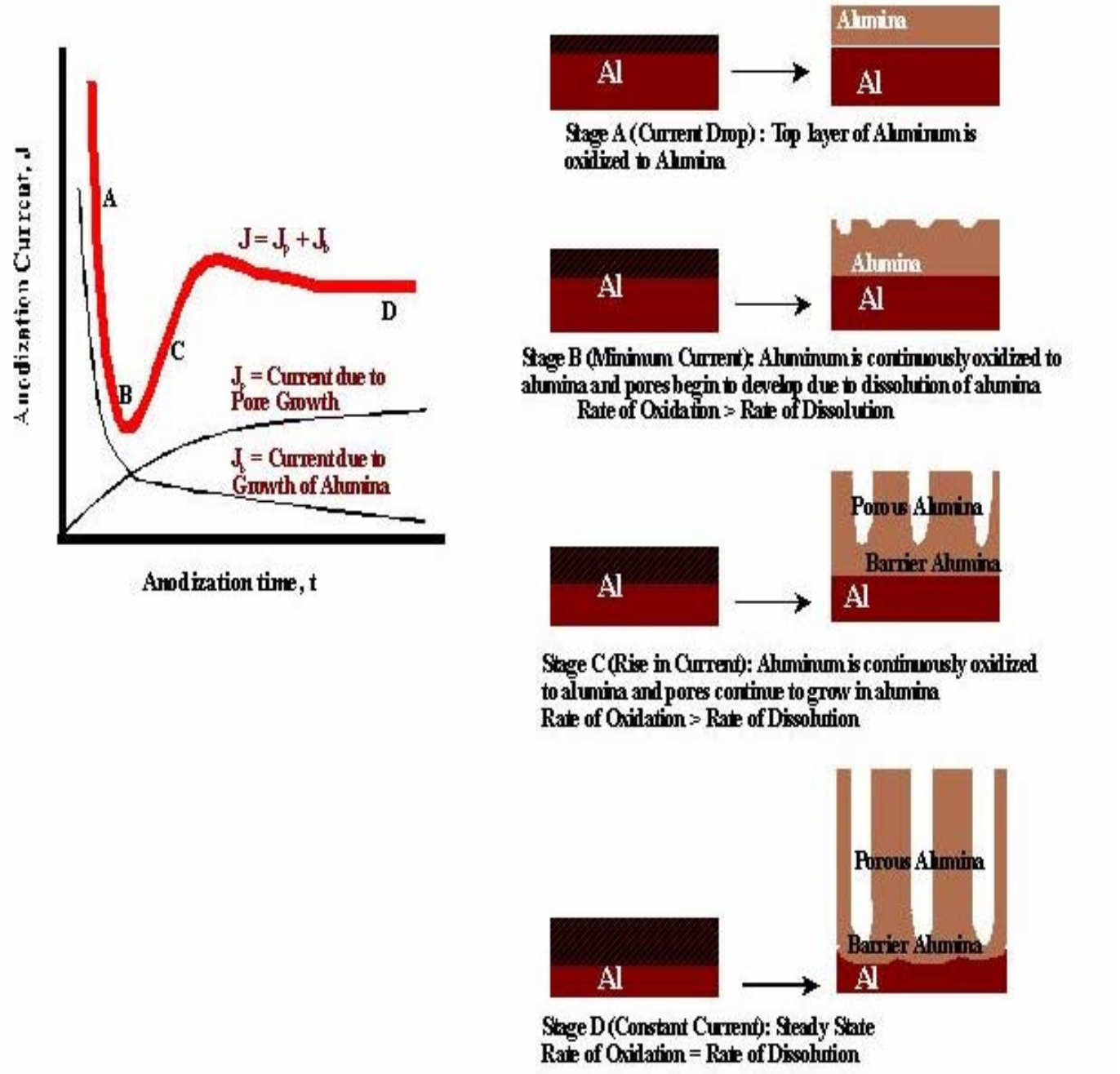

Fig 2.3: Schematic diagram of current density in various stages of the anodization process (Left) and the sequence of pore growth (Right). (Courtesy of Bhargava Kanchibotla PhD Thesis)

As shown in Fig 2.3, during the first few seconds of anodization, the current decreases rapidly until a minimum is reached. This is followed by a slow rise in the anodization current until the steady state is reached. As proposed by O'Sullivan et al, the growth of porous aluminum is a consequence of two competing mechanisms: oxide growth and partial dissolution of the aluminum oxide by the hydrogen ions. Oxide growth is due to the migration of oxygen containing ions O^{2-}/OH^{-} from the electrolyte through the oxide layer to the pore bottom and the dissolution of the oxide is due to the migration of Al^{3+} ions, which drift through the oxide layer and are ejected into the electrolyte. The net current density J can thus be thought of as being a sum of two current contributions, namely, J_b due to the growth of the barrier alumina (which decreases with time) and J_p due to pore growth which increases with time and finally reaches a steady state.

2.5 Multi-step anodization process to fabricate highly ordered porous template

Multi-step anodization is necessary to obtain a highly uniform porous structure. This is because the ordered pore structure is limited to the individual domains of polycrystalline aluminium after the first anodization step.

Following the procedure shown by Masuda et al, the electropolished aluminium coupons were first anodized (15% sulfuric acid for 10 nm pores) for 30 minutes. The sample was then soaked overnight in a wet etchant solution consisting of 25% chromic acid and 5% oxalic in de-ionized water at around 80^{0}C. This completely etches

away the porous membrane and exposes the scalloped surface on top of the aluminum. The second anodization is carried out exactly in the same way as the first but for shorter time duration, 15 mins in case of our samples. The scallops on the aluminum interface now act as the nucleation sites for pore growth. By this method a highly uniform nanoporous template is obtained.

2.6 Transfer of the porous layer onto a glass slide.

As our experiment involves infrared absorption measurements, we will need a substrate that is transparent to near infrared. The aluminum substrate is opaque. Therefore, the porous alumina film has to be released from the substrate and transferred onto a transparent glass slide as a substrate to provide mechanical stability. To accomplish this, the porous layer is smeared with a thin layer of GE varnish and allowed to dry completely. Then an adhesive tape is firmly but gently pressed on the sample such that the glued side sticks on the varnish. The strip of adhesive tape along with the sample is then dipped in a solution of mercuric chloride for at least an hour. This procedure removes the aluminum and it dissolves in the mercuric chloride solution leaving the porous layer attached to the varnish. The tape containing the varnish and porous alumina is then very carefully washed in DI water and wrapped in a thin clean wipe .The whole wrap is then immersed in a Petri dish containing pure ethanol and left to soak overnight. The ethanol dissolves away the varnish and only the porous layer is left sandwiched between the clean wipe layer and the tape. With extreme caution the clean wipe wrap around the tape is gently opened and noting the position of the thin porous alumina layer that portion is pressed onto a clean

glass slide. The ethanol evaporates rapidly and the thin porous film adheres firmly to the glass surface due to surface tension. In this way porous thin film templates of 10nm are prepared.

2.7 Preparation of samples containing one or few organic molecules

These porous films are then soaked in saturated 1, 2-dichloroethane solution of Alq_3 for 24 hours in the dark to allow the organic to fill the pores. There are nanocracks in the pore walls that terminate in 1-2 nm sized nanovoids. Transmission electron microscopy image showing the nanopores with nanocracks of 1-2 nm is displayed in Figure 2.4. The organic molecules diffuse through the cracks and nestle within these nanovoids. Since the size of these nanovoids is barely twice the size of the molecules, only 1 or 2 molecules can fit inside nanovoids.

The films are then soaked for two hours in the solvent only to remove all the excess organic from the pores, leaving behind the molecules trapped in the nanovoids. This happens since the rinsing solution cannot diffuse into the nanovoids and attack the organic molecules trapped there.

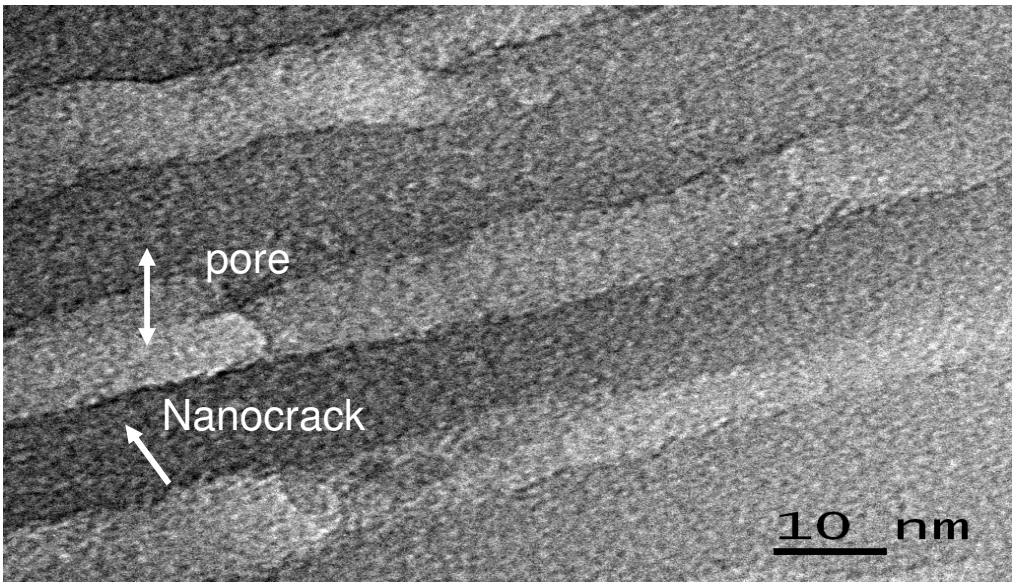

Fig 2.4: TEM cross sectional image of a sample anodized in 15% sulfuric acid at 10V DC. (Courtesy of Bhargava Kanchibotla PhD Thesis)

2.8 Photoluminescence measurement

It is not possible to ascertain with high resolution microscopy that after the rinsing procedure, organic molecules are still left in the nanovoids. Therefore, we carried out room-temperature photoluminescence (PL) measurements on these samples to confirm the presence of the molecules within the nanovoids. Since Alq_3 is optically active, it luminesces in the wavelength range 400 nm – 600 nm, unlike its host (porous alumina produced in sulfuric acid). This allows us to sense the presence of the molecules in the nanocavities. The PL spectrum of porous films containing Alq_3 molecules in nanocavities is shown in Fig. 1. In each case, the PL of blank samples (containing no organics) was subtracted from the PL of organic bearing samples, in order to ascertain that the resulting PL is due to the organics alone.

2.9 FTIR spectroscopy

In Infra-red spectroscopy, radiation in the infra –red region of the spectrum 0.7 and 300 μm is passed through the sample. Each molecule has a unique absorption and transmission spectrum .The absorption peaks correspond to the vibrational frequencies of the atomic bonds making up the material. Thus FTIR is a very precise non-destructive method for qualitative and quantitative analysis of materials and the absorption spectrum is a fingerprint of the molecule.

In our laboratory we used a BOMEM MB104 far infrared FTIR Spectrometer for our experiment. The data from the bulk samples were collected first. For this a clean and empty quartz cuvette was mounted in the path of the beam and the background spectrum was taken. The background spectrum is collected to have a relative scale which is then compared to the spectrum with the sample in the beam to obtain a resulting spectrum which is characteristic of the molecule.

A slight quantity of Alq3 powder is then taken and smeared on the wall of the cuvette with a spatula and absorption and transmittance measurements of the bulk specimen is conducted.

Finally, mid-infrared (IR) absorption spectra Alq_3 molecules confined within nanocavities were measured using Fourier transform infrared (FTIR) spectroscopy. Since a single sample did not produce enough absorption to be detected by our equipment with adequate signal-to-noise ratio, we had to stack three samples to measure absorption. Each sample has a pore density of 10^{12} cm^{-2}, and assuming that each pore has at least one

nanocrack and each such nanocrack has at least 1 molecule, the molecular density will be $\geq 10^{12}$ cm^{-2}. Since our infrared spot size is ~ 1 cm^2, we are sampling the absorption of ~ 3×10^{12} molecules if the above assumptions are reasonable. In all cases, the absorption spectra were obtained by subtracting the spectrum of blank samples (that do not contain any organics, but are otherwise nominally identical with organic bearing samples) from the latter, so that the observed absorption is always due to the organic molecules in the nanocavities alone. The spectrum was averaged over a large number of scans to ensure that it was independent of the number of scans.

CHAPTER 4 Results and Discussion

4.1 Photoluminescence

The obtained PL spectrum is given in Figure 3.1. It has three peaks: at 497 nm, 516 nm and 536 nm, corresponding to photon energies of 2.48 eV, 2.39 eV and 2.30 eV. There is also a broad shoulder at 480 nm. The peak at 497 nm is due to direct transition across the HOMO-LUMO gap and was also observed in refs. 12 and 13 which measured the PL spectrum of Alq_3 molecules trapped in porous alumina prepared in sulfuric acid. This gives us confidence that the organic molecules are present in the nanovoids and have not been removed by the rinsing procedure. Transmission electron microscopy in ref. 5 had ascertained that there are no Alq_3 molecules left outside the nanocavities either. Therefore, the only places occupied by the Alq_3 molecules are the nanocavities.

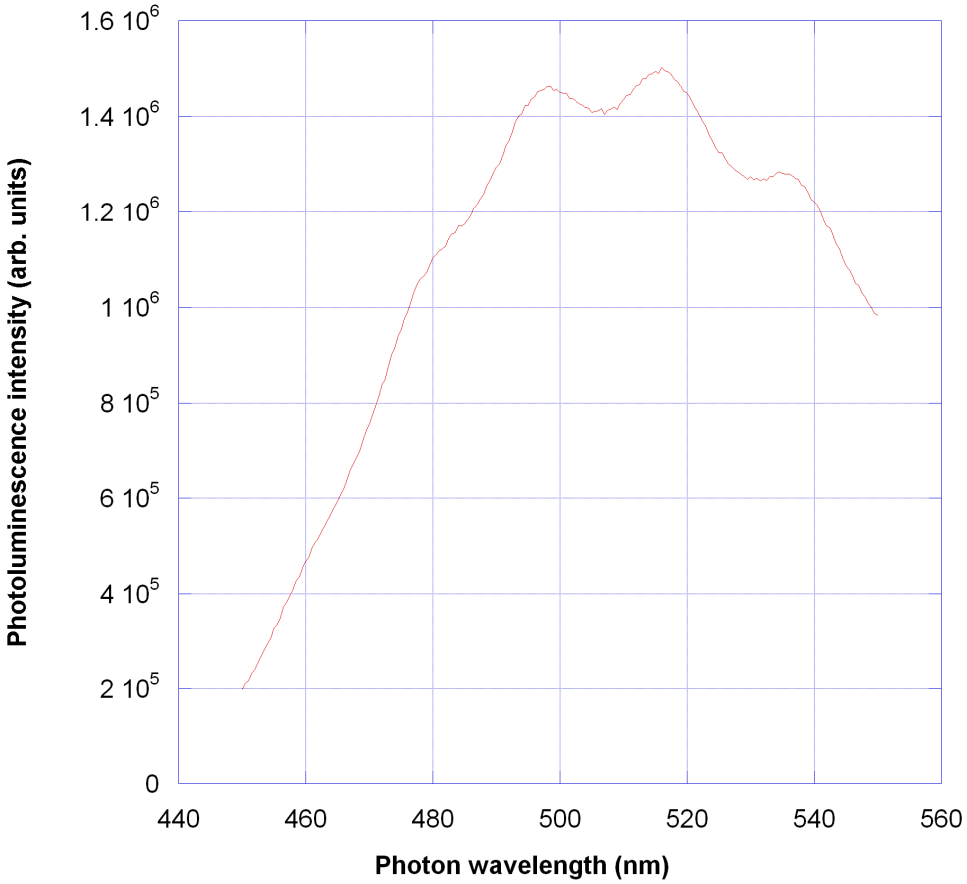

Figure 3.1: Photoluminescence spectra of Alq3 in nanocavities.

The shoulder at 480 nm was barely observed in ref. 12 and not at all in ref. 13. Neither ref. 12, nor ref. 13, observed the lower frequency peaks at 516 nm and 536 nm. All the three low frequency peaks are equally spaced in energy (separation = 90 meV), but they are probably due to impurities that form states in the HOMO-LUMO gap.

4.2 Fourier Transform Infrared Spectroscopy

The IR absorption spectrum of Alq_3 clusters in nanocavities is shown in Fig. 3.2(b). For comparison, we have plotted the IR spectrum of bulk Alq_3 powder in this range in Fig. 3.2(a). Note that the bulk powder's absorption increases monotonically with energy and we see the characteristic peak due to C=H bond stretching. There are a few other peaks in the bulk powder, probably due to impurities. On the other hand, the spectrum of clusters in the nanocavity is *non-monotonic* and shows a very broad peak. The peak and non-monotonic behavior is due to rapid suppression of the absorption above wavenumbers of 3400 cm^{-1}. Pure Alq3 molecule does not have characteristic absorption peaks in the range 3400 – 4000 cm^{-1} due to rotational or vibrational motion, but the bulk powder still shows strong absorption in this range, which may be due to formation of dimers and multimers. This absorption is absent in the clusters.

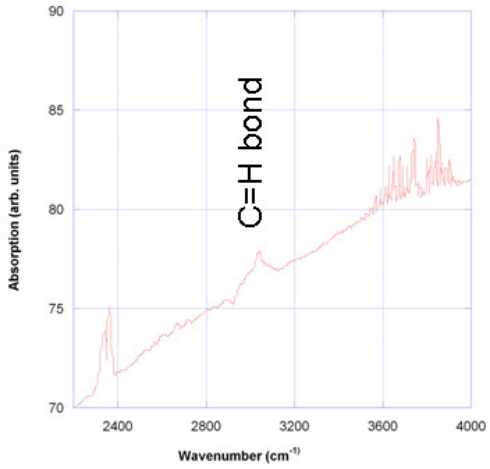

(a)

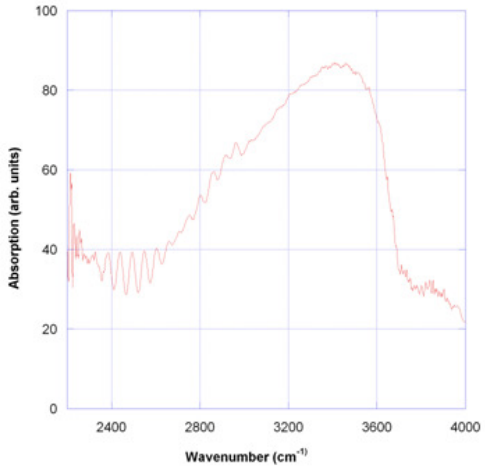

(b)

Figure 3.2: FTIR spectra of (a) bulk and (b) Alq3 in nanocavities.

CHAPTER 4 Conclusion

In conclusion, we have shown that confining an organic molecule within a nanocavity affects its vibrational modes in the mid-infrared range. This is most likely due to boundary conditions imposed by the walls of the nanocavity. If the molecules are physisorbed or chemisorbed on the walls of the cavity, their vibrational and rotational motions will be restricted by the cavity walls, which will alter the rotational and vibrational spectrum. The new rotational and vibrational frequencies could be dependent on the cavity size and the distribution in the cavity size is causing the broad peak (inhomogeneous broadening) in Fig. 2. Finally such modification of the vibrational motion could be a cause for the observed increase in the temperature-dependent spin dephasing time when the Alq_3 molecule is trapped within a nanocavity. While our studies do not rule out other possible mechanisms for the increase in the spin dephasing time, it firmly establishes that renormalization of vibrational and rotational motion is certainly one possible mechanism.

List of References

List of References

1. S. Pramanik, C-G Stefanita, S. Patibandla, S. Bandyopadhyay, K. Garre, N. Harth and M. Cahay, Nature Nanotechnol., **2**, 216 (2007)
2. P. A. Bobbert, W. Wagemans, F. W. A. van Hoost, B. Koopman and M. Wohlgenannt, Phys. Rev. Lett., **102**, 156604 (2009).
3. S. Bandyopadhyay, Phys. Rev. B., **81**, 153202 (2010).
4. S. Sanvito, Nature Mater., **6**, 803 (2007).
5. B. Kanchibotla, S. Pramanik, S. Bandyopadhyay and M. Cahay, Phys. Rev. B., **78**, 193306 (2008).
6. W. J. M. Nabor, S. Faez and W. G. van der Wiel, J. Phys. D: Appl. Phys., **40**, R205 (2007).
7. *Organic Spintronics*, Ed. Z. V. Vardeny (CRC Press, Boca Raton, 2010).
8. M. N. Grecu, A. Mirea, C. Ghica, M. Colle and M. Schwoerer, J. Phys.: Condens. Matter, **17**, 6271 (2005) and references therein.
9. J. Lehmann, A. Arino-Gaita, E. Coronado and D. Loss, Nature Nanotechnol., **2**, 312 (2007).
10. G. S. Huang, X. L. Wu, Y. Xie, F. Kong, Z. Y, Zhang, G. G. Siu and P. K. Chu, Appl. Phys. Lett., **87**, 151910 (2005), and references therein.
11. H. Bensity, C. M. Sotomayor-Torres and C. Weisbuch, Phys. Rev. B., **44**, 10945 (1991).

12. T. Gavrilko, R. Federovich, G. Dovbeshko, A. Marchenko, A. Naumovets, V. Nechytaylo, G. Puchokovska, L. Viduta, J. Baran and H. Ratajczak, J. Mol. Struct., **704**, 163 (2004).
13. S. Bandyopadhyay, A. E. Miller, H-C Chang, G. Banerjee, V. Yuzhakov, D-F Yue, R. E. Ricker, S. Jones, J. A. Eastman, E. Baugher and M. Chandrasekhar, Nanotechnology, **7**, 360 (1996).
14. D. D. Macdonald, J. Electrochem. Soc., **140**, L27 (1993).
15. S. Ono, H. Ichinose and N. Masuko, J. Electrochem. Soc., **138**, 3705 (1991).

VITA

EDUCATION:

M.S. in Electrical and Computer Engineering 2010
Virginia Commonwealth University, Richmond, VA

M.Tech. in Engineering 2004
Jadavpur University, Kolkata, India

B.Tech. in Engineering 2002
University of Kalyani, West Bengal, India

EXPERIENCE:

Graduate Research Assistant 01/2008 – 08/2009
Quantum Device Laboratory-VMC, VCU, Richmond, VA

Graduate Teaching Assistant 08/2009 – 08/2010
Department of Electrical Engineering

Lecturer 06/2005 – 12/2007
West Bengal University of Technology, India

Research Assistant 06/2004 – 06/2005
IC Research Center, ETCE Department
Jadavpur University, India

PUBLICATIONS:

"Improved contacts on a porous silicon layer by electroless nickel plating and copper thickening", J Kanungo , C Pramanik , S Bandopadhyay , U Gangopadhyay , ***L Das*** , H Saha and Robert T T Gettens , *Semicond. Sci. Technol.* **21** 964